該当なし

G．研究発表

１．論文発表

1. Miyazaki O, Nishimura G, Kagami M, Ogata T. Radiological evaluation of dysmorphic thorax of paternal uniparental disomy14. *Pedatric Radiol* (in press)

２．学会発表

1. Osamu Miyazaki, Gen Nishimura, Masayo Kagami, Tsutomu Ogata. Radiological evaluation of dysmorphic thorax in paternal uniparental disomy 14 53rd annual meeting Society for Pediatric Radiology 2011 Boston USA.

H．知的財産権の出願・登録状況

（予定を含む。）

1．特許取得

該当なし

2．実用新案登録

該当なし

3．その他

厚生労働科学研究費補助金（難治性疾患克服研究事業）
分担研究報告書

14番染色体父親性ダイソミーおよび類縁疾患の診断・治療指針の作成

研究分担者　鏡　雅代（独)国立成育医療研究センター研究所　上級研究員

研究要旨

遺伝子診断により確定診断された31症例の臨床像の解析に基き、14番染色体父親性ダイソミーおよび類縁疾患の診断基準および治療のてびきを作成した。この診断基準や治療のてびきの周知により、妊娠中からの適切な母体管理、分娩時期の決定、急性期の治療、長期予後の改善が期待される。

共同研究者

松原圭子（(独)国立成育医療研究センター研究所分子内分泌研究部）
加藤芙弥子（(独)国立成育医療研究センター研究所分子内分泌研究部）
佐藤智子（(独)国立成育医療研究センター研究所分子内分泌研究部）

A. 研究目的

14 番染色体片親性ダイソミー (upd(14)pat) は胎児期より羊水過多、胎盤過成長を呈し出生後はベル型と形容される小胸郭、臍帯ヘルニアなどの腹壁の異常、特徴的な顔貌などを示すが、その疾患概念は、ほとんど浸透していない。upd(14)pat および類縁疾患は 14 番染色体長腕 32.2 領域に存在するインプリンティング遺伝子群の発現異常により生じることが明らかとなっており、遺伝学的病因は、14 番染色体のダイソミー、インプリンティング調節領域を含む微小欠失、インプリンティング調節領域であるメチル化可変領域のメチル化異常によるエピ変異である。本疾患の診断には遺伝子診断が必須であり、その遺伝子診断法は、昨年度に我々によって確立された。本年度は、遺伝子解析により、本疾患群であると確定診断された症例の主治医に対して行った詳細な二次調査結果をもとに、妊娠中経過、新生児期、乳児期の経過、その後の発達障害などの臨床像を明らかとし、診断基準、治療のてびきを作成することを目的とする。

B. 研究方法

診断・治療指針の作成：遺伝子解析にて、14 番染色体父親性ダイソミーおよび類縁疾患であると診断された 31 例について、胎児期、新生児期、乳児期以降の臨床像についての詳細な二次調査を行った。その結果に基づき、upd(14)pat および類縁疾患の診断基準および治療のてびきを作成する。また、長期フォローアップ体制のあり方を提言する。

（倫理面への配慮）

使用したサンプルはすべて（独）国立成育医療研究センター倫理委員会の承認を得たうえで行われている。遺伝子解析は十分なインフォームドコンセントの後に文書により承諾を得た。自験例における臨床情報は全ての個人情報は潜在化させ、個人情報の取り扱いには十分な注意を払っている。

C. 研究結果

昨年度行った一次調査で upd(14)pat 表現型を示す患者の報告例のうち遺伝子診断にて確定された症例 31 人の遺伝学的病因は、ダイソミーが 19 人 (61%)、微小欠失が 7 人 (23%)、エピ変異が 4 人(13%)、不明 1 人 (3%)と判明した。患者主治医に対し、詳細な患者臨床像の調査の結果は、分担研究者柴崎、左合、黒澤の報告に記した。これらの結果をもとに、診断基準、治療のてびきを作成した。

さらに、宮嵜による患者胸部レントゲン写真像の評価により本疾患の画像診断法を作成した。

診断基準

臨床診断基準

主症状

- 妊娠中期より認められる羊水過多
- 胎盤過形成
- 特徴的な小胸郭（コートハンガー型、ベル型）と呼吸障害
- 腹壁の異常（臍帯ヘルニア、腹直筋離開）
- 特徴的顔貌（前額部突出、眼瞼裂狭小、平坦な鼻梁、前向き鼻孔、突出した人中、小顎、鞍状の口唇、小耳）

副症状

- 発達遅延
- 経口摂取障害
- 翼状頚・短頚
- 喉頭軟化症
- 関節拘縮
- 側弯症
- 鼠径ヘルニア

画像診断基準

新生児期はベル型の小胸郭、コートハンガー型肋骨変形の診断的価値が高い。新生児期をすぎるとベル型胸郭が改善するため、診断的価値は低下するが、コートハンガー型肋骨変形は改善傾向がなく診断的価値が高い。

治療てびき（案）

現時点において、治療は対症療法となる。

① 胎児期

羊水過多をきたすため安静入院、子宮収縮抑制剤投与などの早産管理が必要となる。羊水過多が著明で母体の圧迫症状などがでることも多く、適宜羊水吸引術を施行する。できるだけ満期まで妊娠継続する。

② 新生児期

呼吸障害：出生時からほとんどの症例で人工呼吸器管理を必要とする重症の呼吸障害を呈する。一方で酸素投与のみで症状が軽快する軽症例も少ないが存在する。呼吸障害の重症度が生命予後に大きく関与する。呼吸障害の改善に長い時間を必要とする症例が多いが，急性期をのりきれば成長に伴って改善する場合も多い。呼吸障害の原因となる喉頭軟化，気管・気管支軟化，胸郭低形成に対し根本的な治療はなく，成長に伴って改善するのを待機するしかないため、数ヶ月の人工呼吸器、1 年程度の酸素使用（特異に夜間）を必要とすることが多い。

腹壁異常：臍帯ヘルニアは出生時より問題となる。外科手術を必要とするが，臍帯ヘルニアの還納により腹圧が上昇し，呼吸障害が悪化する可能性があり注意が必要である。

③ 乳児期以降

呼吸障害：在宅人工呼吸器で退院する症例も存在する。人工呼吸器からの離脱に関しては、気管気管支軟化症のほかに、胸郭の成長が極めて重要であり、胸郭発達を促す方法としての早期からの呼吸リハビリテーションの導入は極めて重要である。

発達障害：呼吸障害の程度による発達予後は異なるが、重症呼吸管理を必要とした症例においても、適切な呼吸管理下での療育参加などが、長期的な発達予後改善を促す。行動面では、社会性獲得がよく進む症例から、自閉傾向や物事へのこだわりが目立つ症例も認め、専門的評価が必要である。

排便障害：腹壁の異常に起因すると考えられる排便障害に対しては、浣腸、ラキソベロンなどの緩下投与を行う。

経口摂取障害：経管栄養を必要とする症例がおおく、3 歳ころまでの経管栄養、胃ろうを必要とする症例を認める。経口摂取が進まない症例については、摂食リハビリを考慮する。

④その他

2 例に肝芽腫発症を認めており、注意が必要である。

D. 考察

14 番染色体父親性ダイソミーおよびその類縁疾患の診断基準、治療指針は存在しなかった。診断基準に関しては約 30 症例からの臨床情報を得ることができた。結果、5 つの主症状と 7 つの副症状を提案した。特に、主症状である羊水過多、胎盤過形成、ベル型の小胸郭、腹壁異常（特に臍帯ヘルニア）は胎児期にエコーにて同定することが可能であり、適切な母体の管理、出生直後から生じる児の呼吸障害への準備を可能とすることから、産科医、新生児科医へのさらなる啓蒙が必要であろう。本年度はまだデータ数が十分とは

いえないが、長期予後についてのデータも得られ、その臨床像が明らかとなった。重要な点としては、①新生児期の呼吸障害が生命予後を大きく左右すること。②呼吸障害の重症度により発達予後は異なるが、人工呼吸管理下での療育参加が発達予後を促すこと。③排便障害を認める症例が多く、浣腸、緩下剤を適時投与する必要がある。④経口摂取が進まない症例が多く、長期経管栄養を必要とする症例に対しては、摂食リハビリの必要性を示唆する。以上のように、治療は対症療法中心となるが、適切な治療を行うことにより、児の長期予後、生活の質の向上が期待できる。

E. 結論

14 番染色体父性片親性ダイソミー関連疾患の診断基準、治療のてびきを提案した。

F. 健康危険情報

該当なし

G. 研究発表

1．論文発表

1. Kagami M, J O'Sullivan M, Green AJ, Watabe Y, Arisaka O, Masawa N, Matsuoka K, Fukami M, Matsubara K, Kato F, Ferguson-Smith AC, Ogata T. The IG-DMR and the *MEG3*-DMR at Human Chromosome 14q32.2: Hierarchical Interaction and Distinct Functional Properties as Imprinting Control Centers. *PLoS Genetics* 6 (6): e1000992, 2010.
2. Suzumori N, Ogata T, Mizutani E, Hattori Y, Matsubara K, Kagami M, Sugiura-Ogasawara M. Prenatal findings of paternal uniparental disomy 14: Delineation of further patient. *American Journal Medical Genetics A.* 152A (12): 3189–3192, 2010.
3. Yamazawa K, Nakabayashi K, Kagami M, Satoh T, Hata K, Saitoh S, Nagai T, Horikawa R, Hizuka N, Ogata T. A Parthenogenetic Female with a Silver-Russell Syndrome-like Phenotype and a 45,X Cell Lineage Accompanied by Biparentally Derived Autosomes. *Journal of Medical Genetics* 47 (11): 782–785, 2010.
4. 鏡雅代, 細木華奈, 加藤芙弥子, 西村 玄, 斎藤伸治, 緒方勤. 14 番染色体母性片親性ダイソミーは Prader-Willi 症候群の鑑別疾患である. ホルモンと臨床 57 (12): 1069–1076, 2009.

2. 学会発表

1. Masayo Kagami, Maureen J O'Sullivan, Andrew J Green, Yoshiyuki Watabe, Osamu Arisaka, Toshiro Nagai, Shuji Takada, Maki Fukami, Kazuki Yamazawa, Keiko Matsubara, Fumiko Kato, Anne C Ferguson-Smith & Tsutomu Ogata. Hierarchical interaction and distinct functional properties of the IG-DMR and the MEG3-DMR at the human chromosome 14q32.2 imprinted region. 14th International Congress of Endocrinology, Kyoto, 2010.
2. Masayo Kagami, Maureen J O'Sullivan, Andrew J Green, Yoshiyuki Watabe , Osamu Arisaka, Toshiro Nagai, Shuji Takada, Maki Fukami, Kazuki Yamazawa, Keiko Matsubara, Fumiko Kato, Anne C Ferguson-Smith & Tsutomu Ogata. Hierarchical interaction and distinct functional properties of the IG-DMR and the MEG3-DMR at the human chromosome 14q32.2 imprinted region. International Snmposium on Pediatric Endocrinology, Tokyo, 2010.
3. 鏡雅代、高田修治、加藤芙弥子、Anne C Ferguson-Smith、緒方勤. ヒト 14q32.2 のインプリンティング領域において、IG-DMR と MEG3-DMR は異なった役割をはたす. 第 4 回エピジェネティクス研究会、鳥取、2010.
4. 鏡雅代、加藤芙弥子、宮戸真美、高田修治、松岡健太郎、山中美智子、金子さおり、松原圭子、佐藤智子、緒方勤. 14 番染色体インプリンティング遺伝子の胎盤における機能の解明. 第 44 回日本小児内分泌学会学術集会、大阪、2010
5. 鏡雅代 ヒト 14 番染色体インプリンティング異常症発症機序の解明、第 55 回日本人類遺伝学会奨励賞受賞講演、大宮、2010.
6. 鏡雅代、加藤芙弥子、松原圭子、佐藤智子、緒方勤.

14 番染色体父親性ダイソミー症候群の病因別頻度の解明. 第 55 回日本人類遺伝学会学術集会、大宮、2010.

7. Masayo Kagami, Maureen J O'Sullivan, Andrew J Green, Yoshiyuki Watabe, Osamu Arisaka, Nobuhide Masawa, Kentarou Matsuoka, Maki Fukami, Keiko Matsubara, Fumiko Kato, Anne C Ferguson-Smith, and Tsutomu Ogata. The IG-DMR and the *MEG3*-DMR at Human Chromosome 14q32.2: Hierarchical Interaction and Distinct Functional Properties as Imprinting Control Centers, International Symposium on Epigenome Network, Development and Reprograming of Germ Cells, Fukuoka, 2010.
8. Masayo Kagami, Kentaro Matsuoka, Keiko Matsubara, Tomoko Sato, Michiko Yamanaka, Nobuhiro Suzumori, Tsutomu Ogata. *RTL1* plays a key role in human placental development. International Symposium on Epigenome Network, Development and Reprograming of Germ Cells, Fukuoka, 2010.

H. 知的財産権の出願・登録状況

（予定を含む。）

1. 特許取得

該当なし

2. 実用新案登録

該当なし

3. その他

厚生労働科学研究費補助金（難治性疾患克服研究事業）
分担研究報告書

14 番染色体母性片親性ダイソミー関連疾患の遺伝子診断法の確立と日本での実態

研究分担者 齋藤 伸治 北海道大学病院小児科講師

研究要旨

14番染色体母性片親性ダイソミー（upd(14)mat）および関連疾患の遺伝子診断法を確立した。upd(14)matは日本において十分に診断されていない可能性が高いので、実態を知ることを目的として、全国調査を実施した。全国の小児内分泌学会学会員、小児神経学会学会員合計2206名に対して行った一次調査では、825名から回答を得て、135例の表現型陽性例の報告を認めた。日本においてもupd(14)mat関連疾患が疑われる例は多く存在するので、体系的な遺伝子診断法の実施が望まれる。

A．研究目的

14 番染色体母性片親性ダイソミー（upd(14)mat）は子宮内胎児発育遅延、成長障害、新生児期乳児期の筋緊張低下、思春期早発傾向などを示す症候群である。upd(14)mat は 14q32.2 に位置するインプリンティング遺伝子の発現異常により起こることが明らかにされている。この発現異常は upd(14)mat 以外に、同領域の父性欠失、インプリンティング機構の変異であるエピ変異により引き起こされ、同様の症状を示し、upd(14)mat 関連疾患と呼ばれる。したがって、upd(14)mat および関連疾患の診断には系統的な遺伝子診断が必要である。

upd(14)mat および関連疾患の報告例は少数のみである。しかし、発症メカニズムが共通している 15 番染色体母性片親性ダイソミーによって引き起こされる Prader-Willi 症候群（PWS）の発症頻度を考えると、upd(14)mat の大部分は診断されていない可能性が高い。そこで、本研究においては、upd(14)mat および関連疾患の診断のための、系統的な遺伝子診断法の確立と日本における実態の把握を目的とした。

B．研究方法

遺伝子診断法の確立：既に集積済みの検体と新たに収集した検体を対象として、MEG3 メチル化テストにてスクリーニングを行う。メチル化テスト異常例に対しては、多型マーカーを用いた多型解析、同領域に位置する複数のプローブを用いた FISH 解析を実施する。

日本における実態調査：日本小児内分泌学会および日本小児神経学会会員を対象として、アンケート調査を実施し、upd(14)mat および関連疾患の実態を把握する。

（倫理面への配慮）

本研究は国立成育医療研究センターおよび北海道大学大学院医学研究科医の倫理委員会の承認を受け、解析にあたっては、ご家族から書面による同意を得た。

C．研究結果

遺伝子診断法の確立：MEG3 メチル化テスト陽性例 6 例を解析し、upd(14)mat 5 例、エピ変異 1 例を同定した。メチル化テスト陽性例に対して、多型解析、FISH 法の順番で解析を行うことにより、upd(14)mat、微小欠失、エピ変異のすべてを診断できることが示された。

日本小児内分泌学会会員 1183 名および日本小児神経学会会員 1023 名、合計 2206 名を対象として、アンケート用紙を郵送した。その結果、826 名（37.4%）から回答が得られた。その中で、135 例の表現型陽性例が集積された。この 135 例のなかで、遺伝子診断がなされていた例は 30 例であり、それ以外は確定診断がなされていなかった。集積された 135 例に対して、二次調査および、遺伝子診断の提供を提案している。

D．考察

upd(14)mat は子宮内胎児発育遅延、成長障害、新生児期乳児期の筋緊張低下、特徴的な顔貌、思春期早発傾向を示し、特に、成長障害と申請時期乳児期の筋緊張低下にて疑われる。しかし、これらの症状は非特異的であり、診断には遺伝子診断が必須である。私たちは、MEG3 メチル化テスト、多型解析、FISH 解析という系統的な解析法を確立した。分担研究者の結果に加えて、主任研究者の解析結果を合わせると、upd(14)mat、微小欠失、エピ変異のすべての例が適切に同定することができた。したがって、upd(14)mat および関連疾患にたいする遺伝子診断法を確立することができた。

上述したように、upd(14)mat は非特異的な症状を示すので、未診断のままになっている患者が沢山存在することが予想される。upd(15)mat は PWS の表現型を呈し、多数の例が存在することからも、未診断例の存在が指摘されている。一方、upd(14)mat は成長にともない、思春期早発症状効率に示すことが知られており、適切な診断は早期からの適切な対応に結びつく。また、微小欠失例では家族例が知られていることから、遺伝カウンセリングの観点からも適切な診断は重要である。そこで、日本での実態把握のために、アンケート調査を行った。upd(14)mat は成長障害では小児内分泌医が、また、新生児乳児期の筋緊張低下では小児神経医が診察している可能性があるために、両学会に協力を得て、アンケートの対象とした。その結果、135 例の表現型陽性例が抽出された。これまでの確定診断例が 10 例程度であることを考えると、潜在的な患者が多数存在することを示唆する結果と考えられる。現在、二次調査を行うとともに、遺伝子診断の提供を提案しており、これらの抽出された患者にたいする臨床的遺伝学的解析を予定している。

E. 結論

upd(14)mat および関連疾患に対する系統的な遺伝子診断法を確立した。

日本における実態調査を行い、upd(14)mat が疑われる例を 135 例抽出した。upd(14)mat および関連疾患は未診断の状態にある可能性が示唆された。抽出例に対する二次調査を現在行っている。

F．健康危険情報

該当なし

G．研究発表

1．論文発表

1. Nakamura M, Yabe I, Sudo A, Hosoki K, Yaguchi H, Saitoh S, Sasaki H. MERRF/MELAS overlap syndrome: A double pathogenic mutation in mitochondrial tRNA genes. *Journal of Medical Genetics* 47(10):659-664, 2010.
2. Saitsu H, Tohyama J, Kumada T, Egawa K, Hamada K, Okada I, Mizuguchi T, Osaka H, Miyata R, Furukawa T, Haginoya K, Hoshino H, Goto T, Hachiya Y, Yamagata T, Saitoh S, Nagai T, Nishiyama K, Nishimura A, Miyake N, Komada M, Hayashi K, Hirai S, Ogata K, Kato M, Fukuda A, Matsumoto N. Dominant-negative mutations in alpha-II spectrin cause West syndrome with severe cerebral hypomyelination, spastic quadriplegia, and developmental delay. *American Journal of Human Genetics* 86(6):881-891, 2010.
3. Yamazawa K, Nakabayashi K, Kagami M, Satoh T, Hata K, Saitoh S, Nagai T, Horikawa R, Hizuka N, Ogata T. A Parthenogenetic Female with a Silver-Russell Syndrome-like Phenotype and a 45,X Cell Lineage Accompanied by Biparentally Derived Autosomes. *Journal of Medical Genetics* 47 (11): 782–785, 2010.

2．学会発表

1. 斉藤伸治、高橋有美、植田佑樹、伊藤智城、白石秀明：微細染色体異常はプラダー・ウィリー症候群の重要な鑑別診断である、第 52 回日本小児神経学会総会、2010 、福岡
2. 細木華奈、太田亨、新川詔夫、斉藤伸治：PWS 様表現型を示す微細染色体異常、第 55 回日本人類遺伝学会、2010、大宮
3. 細木華奈、太田亨、新川詔夫、斉藤伸治：ゲノム刷り込み関連疾患 Prader-Willi 症候群の表現型を

規定する遺伝学的因子の検討、第 33 回日本分子生物学会年会、2010、神戸

H．知的財産権の出願・登録状況

（予定を含む。）

1．　特許取得

該当なし

2．　実用新案登録

該当なし

3．その他

研究成果の刊行一覧表

雑誌

発表者氏名	論文タイトル名	発表誌名	巻名	ページ	出版年
Kagami M, J O'Sullivan M, Green AJ, Watabe Y, Arisaka O, Masawa N, Matsuoka K, Fukami M, Matsubara K, Kato F, Ferguson-Smith AC, Ogata T.	The IG-DMR and the *MEG3*-DMR at Human Chromosome 14q32.2: Hierarchical Interaction and Distinct Functional Properties as Imprinting Control Centers.	PLoS Genetics	6	e1000992	2010
Miyazaki O, Nishimura G, Kagami M, Ogata T.	Radiological evaluation of dysmorphic thorax of paternal uniparental disomy14.	Pedatric Radiol			(in press)
Suzumori N, Ogata T, Mizutani E, Hattori Y, Matsubara K, Kagami M, Sugiura-Ogasawara M.	Prenatal findings of paternal uniparental disomy 14: Delineation of further patient.	American Journal Medical Genetics A.	152A	3189–3192	2010
Yamanaka M, Ishikawa H, Saito K, Maruyama Y, Ozawa K, Shibasaki J, Nishimura G, Kurosawa K.	Prenatal Findings of Paternal Uniparental Disomy 14: Report of Four Patients.	American Journal Medical Genetics A.	152A	789-791	2010
鏡雅代, 細木華奈, 加藤芙弥子, 西村玄, 斎藤伸治, 緒方勤.	14 番染色体母性片親性ダイソミーは Prader-Willi 症候群の鑑別疾患である.	ホルモンと臨床	57 (12)	1069–1076	2009

研究成果の刊行物・別刷り

The IG-DMR and the *MEG3*-DMR at Human Chromosome 14q32.2: Hierarchical Interaction and Distinct Functional Properties as Imprinting Control Centers

Masayo Kagami[1], Maureen J. O'Sullivan[2], Andrew J. Green[3,4], Yoshiyuki Watabe[5], Osamu Arisaka[5], Nobuhide Masawa[6], Kentarou Matsuoka[7], Maki Fukami[1], Keiko Matsubara[1], Fumiko Kato[1], Anne C. Ferguson-Smith[8], Tsutomu Ogata[1]*

1 Department of Endocrinology and Metabolism, National Research Institute for Child Health and Development, Tokyo, Japan, **2** Department of Pathology, School of Medicine, Our Lady's Children's Hospital, Trinity College, Dublin, Ireland, **3** National Center for Medical Genetics, University College Dublin, Our Lady's Hospital, Dublin, Ireland, **4** School of Medicine and Medical Science, University College, Dublin, Ireland, **5** Department of Pediatrics, Dokkyo University School of Medicine, Tochigi, Japan, **6** Department of Pathology, Dokkyo University School of Medicine, Tochigi, Japan, **7** Department of Pathology, National Center for Child Health and Development, Tokyo, Japan, **8** Department of Physiology, Development and Neuroscience, University of Cambridge, Cambridge, United Kingdom

Abstract

Human chromosome 14q32.2 harbors the germline-derived primary *DLK1-MEG3* intergenic differentially methylated region (IG-DMR) and the postfertilization-derived secondary *MEG3*-DMR, together with multiple imprinted genes. Although previous studies in cases with microdeletions and epimutations affecting both DMRs and paternal/maternal uniparental disomy 14-like phenotypes argue for a critical regulatory function of the two DMRs for the 14q32.2 imprinted region, the precise role of the individual DMR remains to be clarified. We studied an infant with upd(14)pat body and placental phenotypes and a heterozygous microdeletion involving the IG-DMR alone (patient 1) and a neonate with upd(14)pat body, but no placental phenotype and a heterozygous microdeletion involving the *MEG3*-DMR alone (patient 2). The results generated from the analysis of these two patients imply that the IG-DMR and the *MEG3*-DMR function as imprinting control centers in the placenta and the body, respectively, with a hierarchical interaction for the methylation pattern in the body governed by the IG-DMR. To our knowledge, this is the first study demonstrating an essential long-range imprinting regulatory function for the secondary DMR.

Citation: Kagami M, O'Sullivan MJ, Green AJ, Watabe Y, Arisaka O, et al. (2010) The IG-DMR and the *MEG3*-DMR at Human Chromosome 14q32.2: Hierarchical Interaction and Distinct Functional Properties as Imprinting Control Centers. PLoS Genet 6(6): e1000992. doi:10.1371/journal.pgen.1000992

Editor: Wolf Reik, The Babraham Institute, United Kingdom

Received December 29, 2009; **Accepted** May 19, 2010; **Published** June 17, 2010

Funding: This work was supported by grants from the Ministry of Health, Labor, and Welfare; from the Ministry of Education, Science, Sports and Culture; and from Takeda Science Foundation. The funders had no role in study design, data collection and analysis, decision to publish, or preparation of the manuscript.

Competing Interests: The authors have declared that no competing interests exist.

* E-mail: tomogata@nch.go.jp

Introduction

Human chromosome 14q32.2 carries a cluster of protein-coding paternally expressed genes (*PEGs*) such as *DLK1* and *RTL1* and non-coding maternally expressed genes (*MEGs*) such as *MEG3* (alias, *GTL2*), *RTL1as* (*RTL1* antisense), *MEG8*, *snoRNAs*, and *microRNAs* [1,2]. Consistent with this, paternal uniparental disomy 14 (upd(14)pat) results in a unique phenotype characterized by facial abnormality, small bell-shaped thorax, abdominal wall defects, placentomegaly, and polyhydramnios [2,3], and maternal uniparental disomy 14 (upd(14)mat) leads to less-characteristic but clinically discernible features including growth failure [2,4].

The 14q32.2 imprinted region also harbors two differentially methylated regions (DMRs), i.e., the germline-derived primary *DLK1-MEG3* intergenic DMR (IG-DMR) and the postfertilization-derived secondary *MEG3*-DMR [1,2]. Both DMRs are hypermethylated after paternal transmission and hypomethylated after maternal transmission in the body, whereas in the placenta the IG-DMR alone remains as a DMR and the *MEG3*-DMR is rather hypomethylated [1,2]. Furthermore, previous studies in cases with upd(14)pat/mat-like phenotypes have revealed that epimutations (hypermethylation) and microdeletions affecting both DMRs of maternal origin cause paternalization of the 14q32.2 imprinted region, and that epimutations (hypomethylation) affecting both DMRs of paternal origin cause maternalization of the 14q32.2 imprinted region, while microdeletions involving the DMRs of paternal origin have no effect on the imprinting status [2,5–8]. These findings, together with the notion that parent-of-origin specific expression patterns of imprinted genes are primarily dependent on the methylation status of the DMRs [9], argue for a critical regulatory function of the two DMRs for the 14q32.2 imprinted region, with possible different effects between the body and the placenta.

However, the precise role of individual DMR remains to be clarified. Here, we report that the IG-DMR and the *MEG3*-DMR show a hierarchical interaction for the methylation pattern in the body, and function as imprinting control centers in the placenta and the body, respectively. To our knowledge, this is the first study demonstrating not only different roles between the primary and secondary DMRs at a single imprinted region, but also an essential regulatory function for the secondary DMR.

Author Summary

Genomic imprinting is a process causing genes to be expressed in a parent-of-origin specific manner—some imprinted genes are expressed from maternally inherited chromosomes and others from paternally inherited chromosomes. Imprinted genes are often located in clusters regulated by regions that are differentially methylated according to their parental origin. The human chromosome 14q32.2 imprinted region harbors the germline-derived primary *DLK1-MEG3* intergenic differentially methylated region (IG-DMR) and the postfertilization-derived secondary *MEG3*-DMR, together with multiple imprinted genes. Perturbed dosage of these imprinted genes, for example in patients with paternal and maternal uniparental disomy 14, causes distinct phenotypes. Here, through analysis of patients with microdeletions recapitulating some or all of the uniparental disomy 14 phenotypes, we show that the IG-DMR acts as an upstream regulator for the methylation pattern of the *MEG3*-DMR in the body but not in the placenta. Importantly, in the body, the *MEG3*-DMR functions as an imprinting control center. To our knowledge, this is the first study demonstrating an essential function for the secondary DMR in the regulation of multiple imprinted genes. Thus, the results provide a significant advance in the clarification of underlying epigenetic features that can act to regulate imprinting.

Results

Clinical reports

We studied an infant with upd(14)pat body and placental phenotypes (patient 1) and a neonate with upd(14)pat body, but no placental, phenotype (patient 2) (Figure 1). Detailed clinical features of patients 1 and 2 are shown in Table 1. In brief, patient 1 was delivered by a caesarean section at 33 weeks of gestation due to progressive polyhydramnios despite amnioreduction at 28 and 30 weeks of gestation, whereas patient 2 was born at 28 weeks of gestation by a vaginal delivery due to progressive labor without discernible polyhydramnios. Placentomegaly was observed in patient 1 but not in patient 2. Patients 1 and 2 were found to have characteristic face, small bell-shaped thorax with coat hanger appearance of the ribs, and omphalocele. Patient 1 received surgical treatment for omphalocele immediately after birth and mechanical ventilation for several months. At present, she is 5.5 months of age, and still requires intensive care including oxygen administration and tube feeding. Patient 2 died at four days of age due to massive intracranial hemorrhage, while receiving intensive care including mechanical ventilation. The mother of patient 1 had several non-specific clinical features such as short stature and obesity. The father of patient 1 and the parents of patient 2 were clinically normal.

Sample preparation

We isolated genomic DNA (gDNA) and transcripts (*mRNAs*, *snoRNAs*, and *microRNAs*) from fresh leukocytes of patients 1 and the parents of patients 1 and 2, from fresh skin fibroblasts of patient 2, and from formalin-fixed and paraffin-embedded placental samples of patient 1 and similarly treated pituitary and adrenal samples of patient 2 (although multiple body tissues were available in patient 2, useful gDNA and transcript samples were not obtained from other tissues probably due to drastic post-mortem degradation). We also made metaphase spreads from leukocytes and skin fibroblasts. For comparison, we obtained control samples from fresh normal adult leukocytes, neonatal skin fibroblasts, and placenta at 38 weeks of gestation, and from fresh leukocytes of upd(14)pat/mat patients and formalin-fixed and paraffin-embedded placenta of a upd(14)pat patient [2,3].

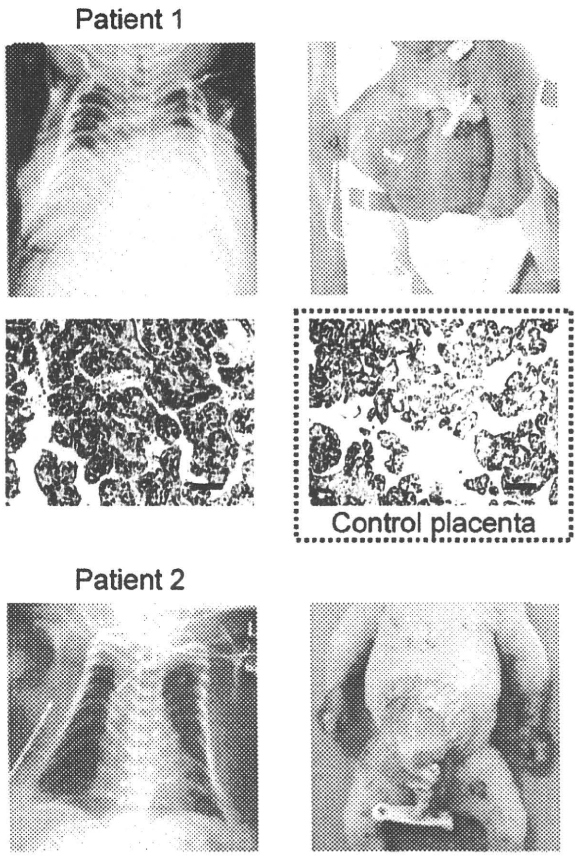

Figure 1. Clinical phenotypes of patients 1 and 2 at birth. Both patients have bell shaped thorax with coat hanger appearance of the ribs and omphalocele. In patient 1, histological examination of the placenta shows proliferation of dilated and congested chorionic villi, as has previously been observed in a case with upd(14)pat [2]. For comparison, the histological finding of a gestational age matched (33 weeks) control placenta is shown in a dashed square. The horizontal black bars indicate 100 μm.
doi:10.1371/journal.pgen.1000992.g001

Structural analysis of the imprinted region

We first examined the structure of the 14q32.2 imprinted region (Figure 2). Upd(14) was excluded in patients 1 and 2 as well as in the mother of patient 1 by microsatellite analysis (Table S1), and FISH analysis for the two DMRs identified a familial heterozygous deletion encompassing the IG-DMR alone in patient 1 and her mother and a *de novo* heterozygous deletion encompassing the *MEG3*-DMR alone in patient 2 (Figure 2). The microdeletions were further localized by SNP genotyping for 70 loci (Table S1) and quantitative real-time PCR (q-PCR) analysis for four regions around the DMRs (Figure S1A), and serial direct sequencing for the long PCR products harboring the deletion junctions successfully identified the fusion points of the microdeletions in patient 1 and her mother and in patient 2 (Figure 2). According to the NT_026437 sequence data at the NCBI Database (Genome Build 36.3) (http://preview.ncbi.nlm.nih.gov/guide/), the deletion

Table 1. Clinical features in patients 1 and 2.

	Patient 1	Patient 2	Upd(14)pat (n = 20)[c]
Present age	5.5 months	Deceased at 4 days	0–9 years
Sex	Female	Female	Male:Female = 9:11
Karyotype	46,XX	46,XX	
Pregnancy and delivery			
Gestational age (weeks)	33	28	28–37
Delivery	Caesarean	Vaginal	Vaginal:Caesarean = 6:7
Polyhydramnios	Yes	No	20/20 (<28)[d]
Amnioreduction (weeks)	2× (28, 30)	No	6/6
Placentomegaly	Yes	No	10/10
Growth pattern			
Prenatal growth failure	No	No	1/13
Birth length (cm)	43 (WNR)[a]	34 (WNR)[a]	
Birth weight (kg)	2.84 (>90 centile)[a]	1.32 (WNR)[a]	
Postnatal growth failure	Yes	…	5/6
Present stature (cm)	56.3 (−3.0 SD)[b]	…	
Present weight (kg)	5.02 (−3.0 SD)[b]	…	
Characteristic face			
Frontal bossing	No	Yes	5/7
Hairy forehead	Yes	Yes	9/10
Blepharophimosis	Yes	No	14/15
Depressed nasal bridge	Yes	Yes	13/13
Anteverted nares	Yes	No	6/10
Small ears	Yes	Yes	11/12
Protruding philtrum	Yes	No	15/15
Puckered lips	No	No	3/10
Micrognathia	Yes	Yes	11/12
Thoracic abnormality			
Bell-shaped thorax	Yes	Yes	17/17
Mechanical ventilation	Yes	Yes	17/17
Abdominal wall defect			
Diastasis recti	…	…	15/17
Omphalocele	Yes	Yes	2/17[e]
Others			
Short webbed neck	Yes	Yes	14/14
Cardiac disease	No	Yes (PDA)	5/10
Inguinal hernia	No	No	2/6
Coxa valga	Yes	No	3/4
Joint contractures	Yes	No	8/10
Kyphoscoliosis	No	No	4/7
Extra features		Hydronephrosis (bilateral)	

WNR: within the normal range; SD: standard deviation; and PDA: patent ductus arteriosus.

a Assessed by the gestational age- and sex-matched Japanese reference data from the Ministry of Health, Labor, and Welfare (http://www.e-stat.go.jp/SG1/estat/GL02020101.do).

b Assessed by the age- and sex-matched Japanese reference data..

c In the column summarizing the clinical features of 20 patients with upd(14)pat, the denominators indicate the number of cases examined for the presence or absence of each feature, and the numerators represent the number of cases assessed to be positive for that feature; thus, the differences between the denominators and the numerators denote the number of cases evaluated to be negative for that feature (adopted from reference [2]).

d Polyhydramnios has been identified by 28 weeks of gestation.

e Omphalocele is present in two cases with upd(14)pat and in two cases with epimutations [2].

doi:10.1371/journal.pgen.1000992.t001

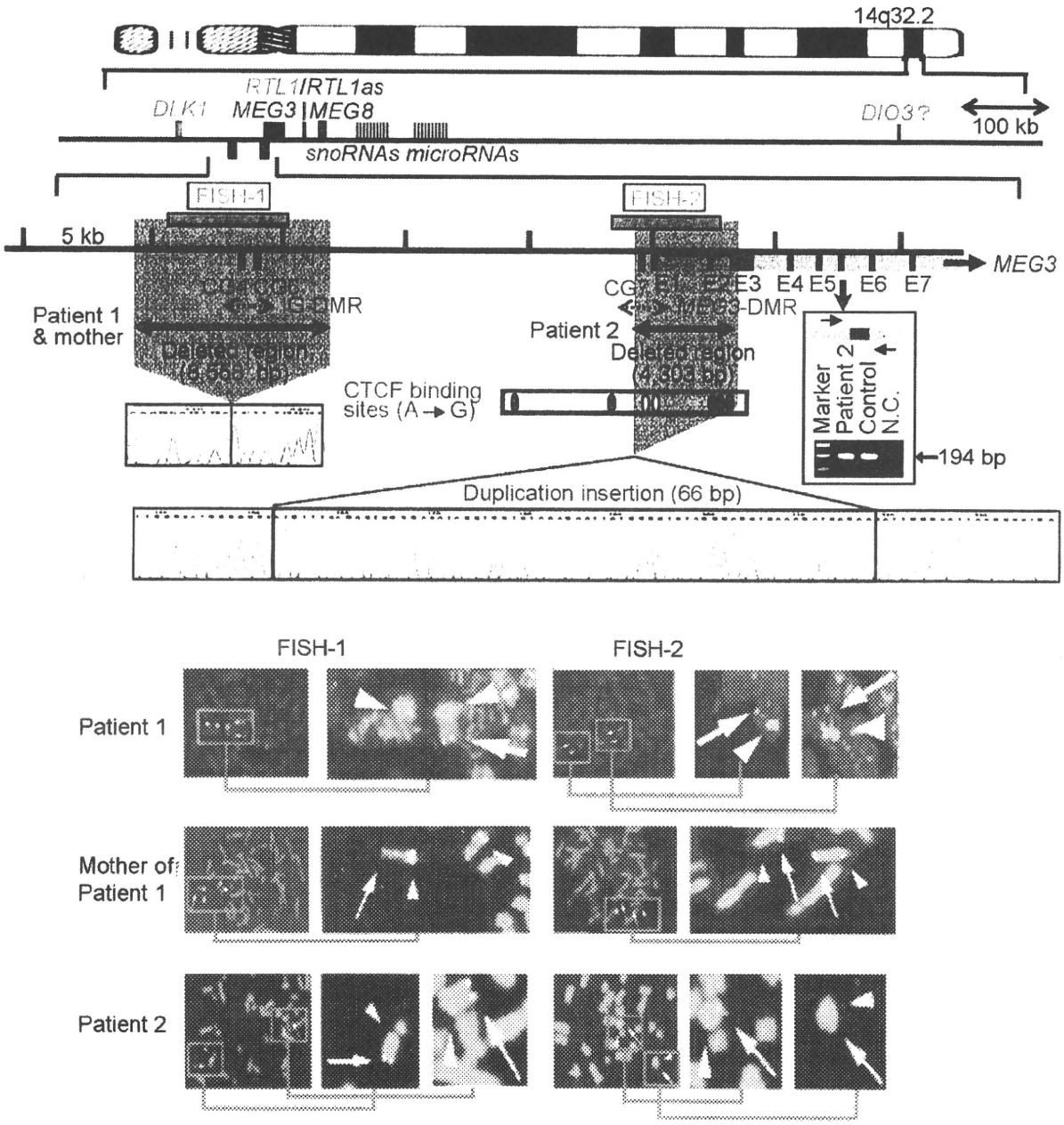

Figure 2. Physical map of the 14q32.2 imprinted region and the deleted segments in patient 1 and her mother and in patient 2 (shaded in gray). *PEGs* are shown in blue, *MEGs* in red, and the IG-DMR (CG4 and CG6) and the *MEG3*-DMR (CG7) in green. It remains to be clarified whether *DIO3* is a *PEG*, although mouse *Dio3* is known to be preferentially but not exclusively expressed from a paternally derived chromosome [35]. For *MEG3*, the isoform 2 with nine exons (red bars) and eight introns (light red segment) is shown (Ensembl; http://www.ensembl.org/index.html). Electrochromatograms represent the fusion point in patient 1 and her mother, and the fusion point accompanied by insertion of a 66 bp segment (highlighted in blue) with a sequence identical to that within *MEG3* intron 5 (the blue bar) in patient 2. Since PCR amplification with primers flanking the 66 bp segment at *MEG3* intron 5 has produced a 194 bp single band in patient 2 as well as in a control subject (shown in the box), this indicates that the 66 bp segment at the fusion point is caused by a duplicated insertion rather than by a transfer from intron 5 to the fusion point (if the 66 bp is transferred from the original position, a 128 bp band as well as a 194 bp band should be present in patient 2) (the marker size: 100, 200, and 300 bp). In the FISH images, the red signals (arrows) have been identified by the FISH-1 probe and the FISH-2 probe, and the light green signals (arrowheads) by the RP11-566I2 probe for 14q12 used as an internal control. The faint signal detected by the FISH-2 probe in patient 2 is consistent with the preservation of a ~1.2 kb region identified by the centromeric portion of the FISH-2 probe.
doi:10.1371/journal.pgen.1000992.g002

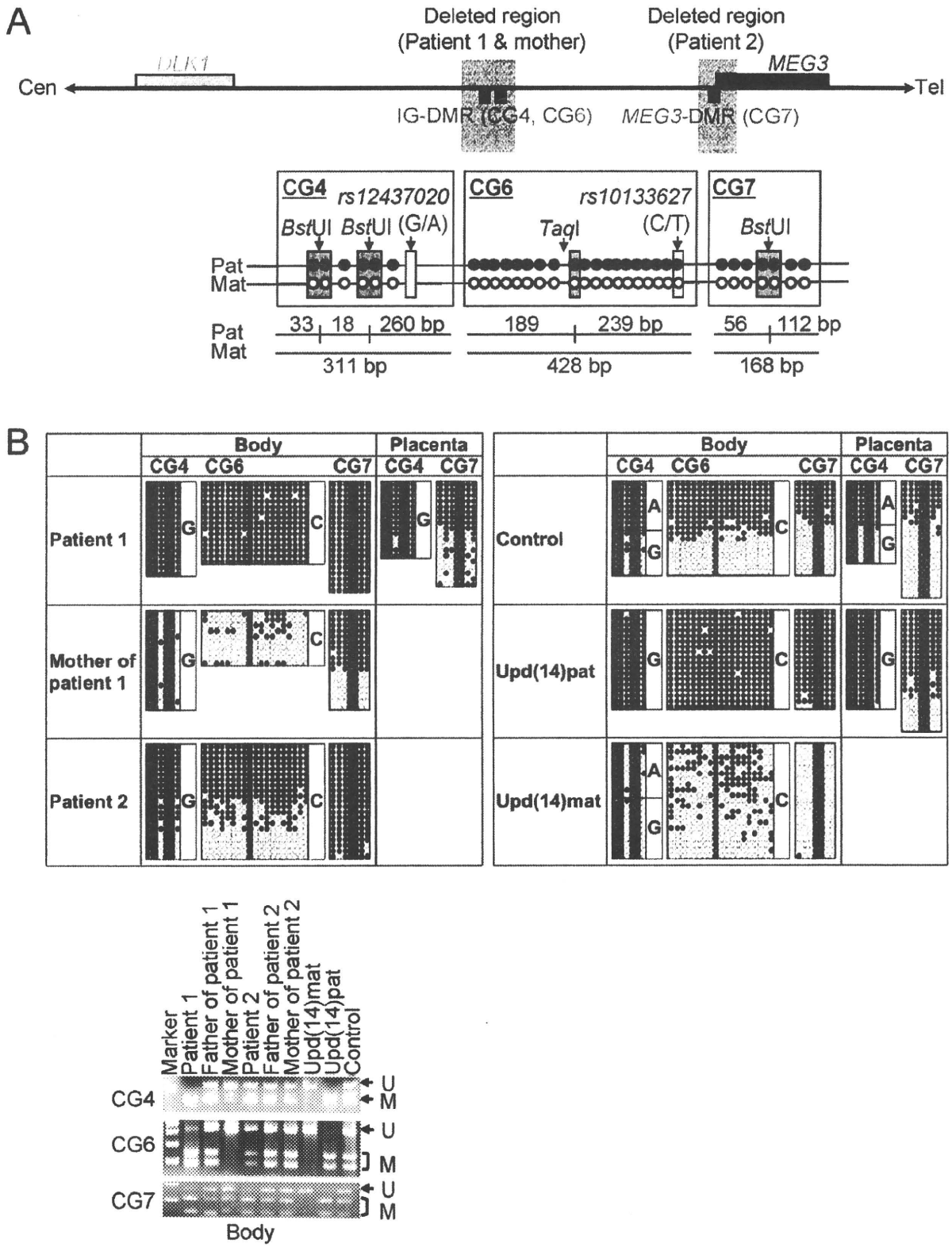

Figure 3. Methylation analysis of the IG-DMR (CG4 and CG6) and the *MEG3*-DMR (CG7). Filled and open circles indicate methylated and unmethylated cytosines at the CpG dinucleotides, respectively. (A) Structure of CG4, CG6, and CG7. Pat: paternally derived chromosome; and Mat:

maternally derived chromosome. The PCR products for CG4 (311 bp) harbor 6 CpG dinucleotides and a G/A SNP (*rs12437020*), and are digested with *Bst*UI into three fragment (33 bp, 18 bp, and 260 bp) when the cytosines at the first and the second CpG dinucleotides and the fourth and the fifth CpG dinucleotides (indicated with orange rectangles) are methylated. The PCR products for CG6 (428 bp) carry 19 CpG dinucleotides and a C/T SNP (*rs10133627*), and are digested with *Taq*I into two fragment (189 bp and 239 bp) when the cytosine at the 9th CpG dinucleotide (indicated with an orange rectangle) is methylated. The PCR products for CG7 harbor 7 CpG dinucleotides, and are digested with *Bst*UI into two fragment (56 bp and 112 bp) when the cytosines at the fourth and the fifth CpG dinucleotides (indicated with orange rectangles) are methylated. These enzymes have been utilized for combined bisulfite restriction analysis (COBRA). (B) Methylation analysis. Upper part shows bisulfite sequencing data. The SNP typing data are also denoted for CG4 and CG6. The circles highlighted in orange correspond to those shown in Figure 3A. The relatively long CG6 was not amplified from the formalin-fixed and paraffin-embedded placental samples, probably because of the degradation of genomic DNA. Note that CG4 is differentially methylated in a control placenta and is massively hypermethylated in a upd(14)pat placenta, whereas CG7 is rather hypomethylated in a upd(14)pat placenta as well as in a control placenta. Lower part shows COBRA data. U: unmethylated clone specific bands (311 bp for CG4, 428 bp for CG6, and 168 bp for CG7); and M: methylated clone specific bands (260 bp for CG4, 239 bp and 189 bp for CG6, and 112 bp and 56 bp for CG7). The results reproduce the bisulfite sequencing data, and delineate normal findings of the father of patient 1 and the parents of patient 2.
doi:10.1371/journal.pgen.1000992.g003

size was 8,558 bp (82,270,449–82,279,006 bp) for the microdeletion in patient 1 and her mother, and 4,303 bp (82,290,978–82,295,280 bp) for the microdeletion in patient 2. The microdeletion in patient 2 also involved the 5′ part of *MEG3* and five of the seven putative CTCF binding sites A–G [10], and was accompanied by insertion of a 66 bp sequence duplicated from *MEG3* intron 5 (82,299,727–82,299,792 bp on NT_026437). Direct sequencing of the exonic or transcribed regions detected no mutation in *DLK1*, *MEG3*, and *RTL1*, although several cDNA polymorphisms (cSNPs) were identified (Table S1). Oligoarray comparative genomic hybridization identified no other discernible structural abnormality (Figure S1B).

Methylation analysis of the two DMRs and the seven putative CTCF binding sites

We next studied methylation patterns of the previously reported IG-DMR (CG4 and CG6) and *MEG3*-DMR (CG7) (Figure 3A) [2], using bisulfite treated gDNA samples. Bisulfite sequencing and combined bisulfite restriction analysis using body samples revealed a hypermethylated IG-DMR and *MEG3*-DMR in patient 1, a hypomethylated IG-DMR and differentially methylated *MEG3*-DMR in the mother of patient 1, and a differentially methylated IG-DMR and hypermethylated *MEG3*-DMR in patient 2, and bisulfite sequencing using placental samples showed a hypermethylated IG-DMR and rather hypomethylated *MEG3*-DMR in patient 1 (Figure 3B).

We also examined methylation patterns of the seven putative CTCF binding sites by bisulfite sequencing (Figure 4A). The sites C and D alone exhibited DMRs in the body and were rather hypomethylated in the placenta (Figure 4B), as observed in CG7. Furthermore, to identify an informative SNP(s) pattern for allele-specific bisulfite sequencing, we examined a 349 bp region encompassing the site C and a 356 bp region encompassing the site D as well as a 300 bp region spanning the previously reported three SNPs near the site D, in 120 control subjects, the cases with upd(14)pat/mat, and patients 1 and 2 and their parents. Consequently, an informative polymorphism was identified for a novel G/A SNP near the site D in only a single control subject, and the parent-of-origin specific methylation pattern was confirmed (Figure 4C). No informative SNP was found in the examined region around the site C, and no other informative SNP was identified in the two examined regions around the site D, with the previously known three SNPs being present in a homozygous condition in all the subjects analyzed.

Expression analysis of the imprinted genes

Finally, we performed expression analyses, using standard reverse transcriptase (RT)-PCR and/or q-PCR analysis for multiple imprinted genes in this region (Figure 5A–5C). For leukocytes, weak expression was detected for *MEG3* and *SNORD114-29* in a control subject and the mother of patient 1 but not in patient 1. For skin fibroblasts, although all *MEGs* but no *PEGs* were expressed in control subjects, neither *MEGs* nor *PEGs* were expressed in patient 2. For placentas, although all imprinted genes were expressed in control subjects, *PEGs* only were expressed in patient 1. For the pituitary and adrenal of patient 2, *DLK1* expression alone was identified.

Expression pattern analyses using informative cSNPs revealed monoallelic *MEG3* expression in the leukocytes of the mother of patient 1 (Figure 5D), and biparental *RTL1* expression in the placenta of patient 1 (no informative cSNP was detected for *DLK1*) and biparental *DLK1* expression in the pituitary and adrenal of patient 2 (*RTL1* was not expressed in the pituitary and adrenal) (Figure 5E), as well as maternal *MEG3* expression in the control leukocytes and paternal *RTL1* expression in the control placentas (Figure S2). Although we also attempted q-PCR analysis, precise assessment was impossible for *MEG3* in the mother of patient 1 because of faint expression level in leukocytes and for *RTL1* in patient 1 and *DLK1* in patient 2 because of poor quality of mRNAs obtained from formalin-fixed and paraffin-embedded tissues.

Discussion

The data of the present study are summarized in Figure 6. Parental origin of the microdeletion positive chromosomes is based on the methylation patterns of the preserved DMRs in patients 1 and 2 and the mother of patient 1 as well as maternal transmission in patient 1. Loss of the hypomethylated IG-DMR of maternal origin in patient 1 was associated with epimutation (hypermethylation) of the *MEG3*-DMR in the body and caused paternalization of the imprinted region and typical upd(14)pat body and placental phenotypes, whereas loss of the hypomethylated *MEG3*-DMR of maternal origin in patient 2 permitted normal methylation pattern of the IG-DMR in the body and resulted in maternal to paternal epigenotypic alteration and typical upd(14)pat body, but no placental, phenotype. In this regard, while a 66 bp segment was inserted in patient 2, this segment contains no known regulatory sequence [11] or evolutionarily conserved element [12] (also examined with a VISTA program, http://genome.lbl.gov/vista/index.shtml). Similarly, while no control samples were available for pituitary and adrenal, the previous study in human subjects has shown paternal *DLK1* expression in adrenal as well as monoallelic *DLK1* and *MEG3* expressions in various tissues [11]. Furthermore, the present and the previous studies [2] indicate that this region is imprinted in the placenta as well as in the body. Thus, these results, in conjunction with the finding that the IG-DMR remains as a DMR and the *MEG3*-DMR exhibits a non-DMR in the placenta [2], imply the following: (1) the IG-DMR functions hierarchically as an upstream regulator for the methylation pattern of the *MEG3*-DMR on the maternally inherited chromosome in the body, but not in the placenta; (2) the hypomethylated

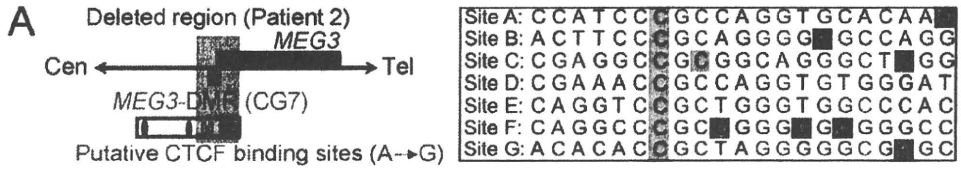
A
Deleted region (Patient 2)
MEG3
Cen
Tel
MEG3-DMR (CG7)
Putative CTCF binding sites (A→G)
Site A: C C A T C C C G C C A G G T G C A C A A
Site B: A C T T C C C G C A G G G G G C C A G G
Site C: C G A G G C C G C G G C A G G G C T G G
Site D: C G A A A C C G C C A G G T G T G G G A T
Site E: C A G G T C C G C T G G G T G G C C C A C
Site F: C A G G C C C G C G G G G G G G C C
Site G: A C A C A C C G C T A G G G G G C G G C

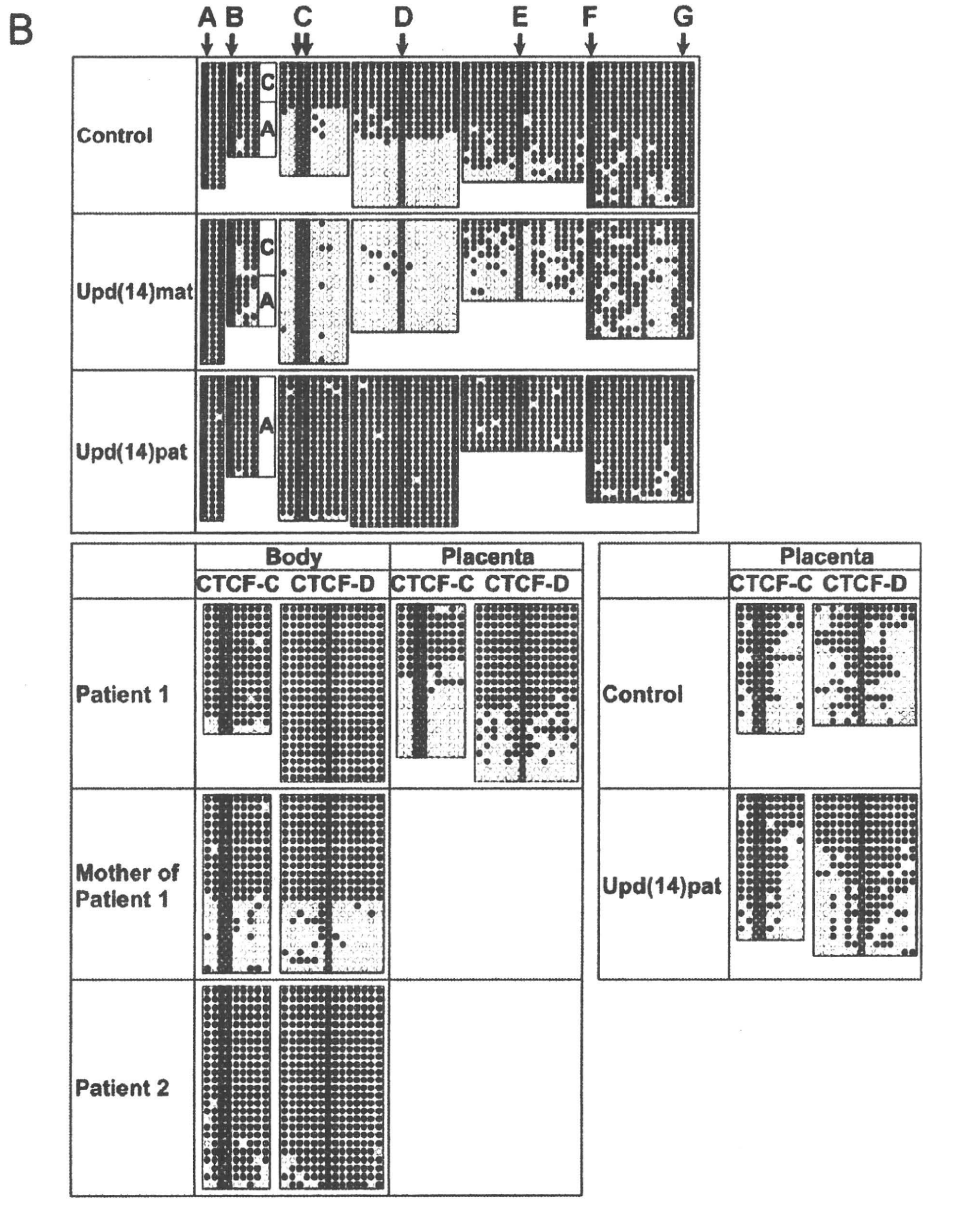
B
A B C D E F G
Control
Upd(14)mat
Upd(14)pat
C
A
Body
Placenta
CTCF-C CTCF-D
CTCF-C CTCF-D
Patient 1
Mother of Patient 1
Patient 2
Placenta
CTCF-C CTCF-D
Control
Upd(14)pat

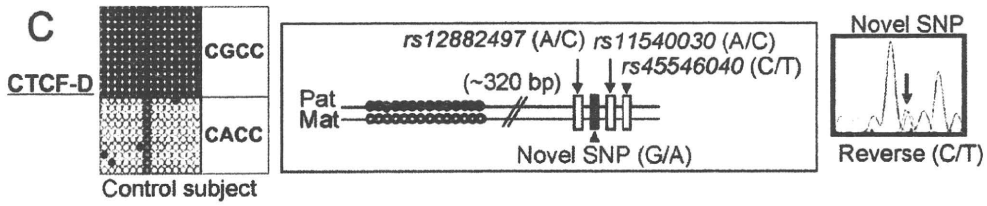
C
CTCF-D
CGCC
CACC
Control subject
rs12882497 (A/C) rs11540030 (A/C)
rs45546040 (C/T)
(~320 bp)
Pat
Mat
Novel SNP (G/A)
Novel SNP
Reverse (C/T)

Figure 4. Methylation analysis of the putative CTCF protein binding sites A–G. (A) Location and sequence of the putative CTCF binding sites. In the left part, the sites C and D are painted in yellow and the remaining sites in purple. In the right part, the consensus CTCF binding motifs are shown in red letters; the cytosine residues at the CpG dinucleotides within the CTCF binding motifs are highlighted in blue, and those outside the CTCF binding motifs are highlighted in green [10]. (B) Methylation analysis. Upper part shows bisulfite sequencing data, using leukocyte genomic DNA samples. Since PCR products for the site B contain a C/A SNP (*rs11627993*), genotyping data are also indicated. The circles highlighted in blue correspond to those shown in Figure 4A. The sites C and D exhibit clear DMRs. Lower part indicates the results of the sites C and D using leukocyte and/or placental genomic DNA samples. The findings are similar to those of CG7. (C) Allele-specific methylation pattern of the CTCF binding site D. A novel G/A SNP has been identified in a single control subject, as shown on a reverse chromatogram delineating a C/T SNP pattern, while the previously reported three SNPs were present in a homozygous condition. Methylated and unmethylated clones are associated with the "G" and the "A" alleles, respectively.
doi:10.1371/journal.pgen.1000992.g004

MEG3-DMR functions as an essential imprinting regulator for both *PEGs* and *MEGs* in the body; and (3) in the placenta, the hypomethylated IG-DMR directly controls the imprinting pattern of both *PEGs* and *MEGs*. These notions also explain the epigenotypic alteration in the previous cases with epimutations or microdeletions affecting both DMRs (Figure S3).

It remains to be clarified how the IG-DMR and the *MEG3*-DMR interact hierarchically in the body. However, the present data, together with the previous findings in cases with epimutations [2,5–8], imply that *MEG3*-DMR can remain hypomethylated only in the presence of a hypomethylated IG-DMR and is methylated when the IG-DMR is deleted or methylated irrespective of the parental origin. Furthermore, mouse studies have suggested that the methylation pattern of the postfertilization-derived *Gtl2*-DMR (the mouse homolog for the *MEG3*-DMR) is dependent on that of the germline-derive IG-DMR [13]. Thus, a preferential binding of some factor(s) to the unmethylated IG-DMR may cause a conformational alteration of the genomic structure, thereby protecting the methylation of the *MEG3*-DMR.

It also remains to be elucidated how the IG-DMR and the *MEG3*-DMR regulate the expression of both *PEGs* and *MEGs* in the placenta and the body, respectively. For the *MEG3*-DMR, however, the CTCF binding sites C and D may play a pivotal role in the imprinting regulation. The methylation analysis indicates that the two sites reside within the *MEG3*-DMR, and it is known that the CTCF protein with versatile functions preferentially binds to unmethylated target sequences including the sites C and D [10,14–16]. In this regard, all the *MEGs* in this imprinted region can be transcribed together in the same orientation and show a strikingly similar tissue expressions pattern [1,12], whereas *PEGs* are transcribed in different directions and are co-expressed with *MEGs* only in limited cell-types [1,17]. It is possible, therefore, that preferential CTCF binding to the grossly unmethylated sites C and D activates all the *MEGs* as a large transcription unit and represses all the *PEGs* perhaps by influencing chromatin structure and histone modification independently of the effects of expressed *MEGs*. In support of this, CTCF protein acts as a transcriptional activator for *Gtl2* (the mouse homolog for *MEG3*) in the mouse [18].

Such an imprinting control model has not been proposed previously. It is different from the CTCF protein-mediated insulator model indicated for the *H19*-DMR and from the non-coding RNA-mediated model implicated for several imprinted regions including the KvDMR1 [19]. However, the KvDMR1 harbors two putative CTCF binding sites that may mediate non-coding RNA independent imprinting regulation [20], and the imprinting control center for Prader-Willi syndrome [21] also carries three CTCF binding sites (examined with a Search for CTCF DNA Binding Sites program, http://www.essex.ac.uk/bs/molonc/spa.html). Thus, while each imprinted region would be regulated by a different mechanism, a CTCF protein may be involved in the imprinting control of multiple regions, in various manners.

This imprinted region has also been studied in the mouse. Clinical and molecular findings in wildtype mice [1,22,23], mice with PatDi(12) (paternal disomy for chromosome 12 harboring this imprinted region) [13,24,25], and mice with targeted deletions for the IG-DMR (ΔIG-DMR) [22,26] and for the *Gtl2*-DMR (Δ*Gtl2*-DMR) [27] are summarized in Table 2. These data, together with human data, provide several informative findings. First, in both the human and the mouse, the IG-DMR is differentially methylated in both the body and the placenta, whereas the *MEG3/Gtl2*-DMR is differentially methylated in the body and exhibits non-DMR in the placenta. Second, the IG-DMR and the *MEG3/Gtl2*-DMR show a hierarchical interaction on the maternally derived chromosome in both the human and the mouse bodies. Indeed, the *MEG3/Gtl2*-DMR is epimutated in patient 1 and mice with maternally inherited ΔIG-DMR, and the IG-DMR is normally methylated in patient 2 and mice with maternally inherited Δ*Gtl2*-DMR. Third, the function of the IG-DMR is comparable between human and mouse bodies and different between human and mouse placentas. Indeed, patient 1 has upd(14)pat body and placental phenotypes, whereas mice with the ΔIG-DMR of maternal origin have PatDi(12)-compatible body phenotype and apparently normal placental phenotype. It is likely that imprinting regulation in the mouse placenta is contributed by some mechanism(s) other than the methylation pattern of the IG-DMR, such as chromatin conformation [22,28,29].

Unfortunately, however, the data of Δ*Gtl2*-DMR mice appears to be drastically complicated by the retained neomycin cassette in the upstream region of *Gtl2*. Indeed, it has been shown that the insertion of a *lacZ* gene or a neomycin gene in the similar upstream region of *Gtl2* causes severely dysregulated expression patterns and abnormal phenotypes after both paternal and maternal transmissions [30,31], and that deletion of the inserted neomycin gene results in apparently normal expression patterns and phenotypes after both paternal and maternal transmissions [31]. (In this regard, although a possible influence of the inserted 66 bp segment can not be excluded formally in patient 2, phenotype and expression data in patient 2 are compatible with simple paternalization of the imprinted region.) In addition, since the apparently normal phenotype in mice homozygous for Δ*Gtl2*-DMR is reminiscent of that in sheep homozygous for the callipyge mutation [32], a complicated mechanism(s) such as the polar overdominance may be operating in the Δ*Gtl2*-DMR mice [33]. Thus, it remains to be clarified whether the *MEG3/Gtl2*-DMR has a similar or different function between the human and the mouse.

Two points should be made in reference to the present study. First, the proposed functions of the two DMRs are based on the results of single patients. This must be kept in mind, because there might be a hidden patient-specific abnormality or event that might explain the results. For example, the abnormal placental phenotype in patient 1 might be caused by some co-incidental aberration, and the apparently normal placenta in patient 2 might be due to mosaicism with grossly preserved *MEG3*-DMR in the placenta and grossly deleted *MEG3*-DMR in the body. Second,

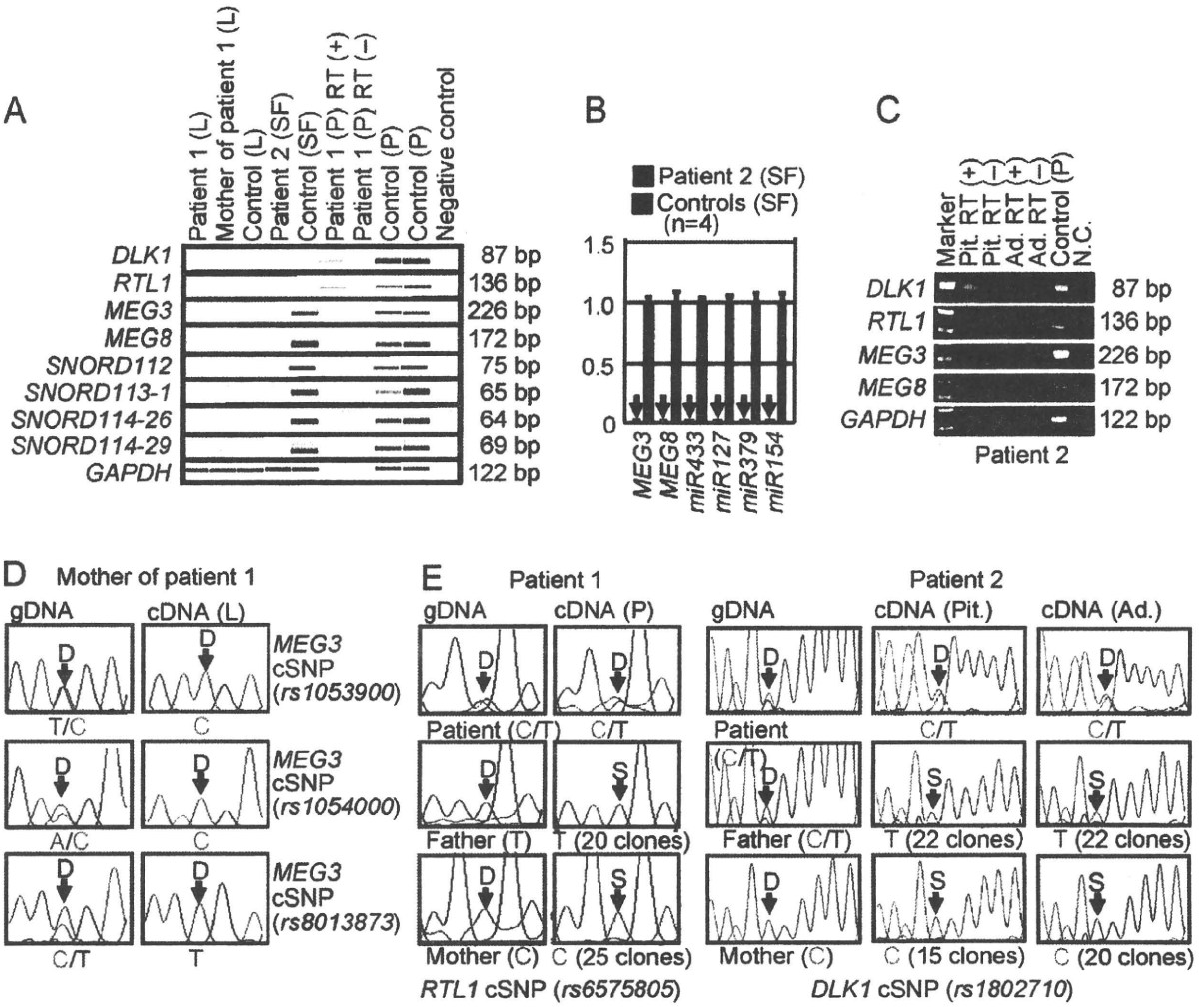

Figure 5. Expression analysis. (A) Reverse transcriptase (RT)-PCR analysis. L: leukocytes; SF: skin fibroblasts; and P: placenta. The relatively weak *GAPDH* expression for the formalin-fixed and paraffin-embedded placenta of patient 1 indicates considerable mRNA degradation. Since a single exon was amplified for *DLK1* and *RTL1*, PCR was performed with and without RT for the placenta of patient 1, to exclude the possibility of false positive results caused by genomic DNA contamination. (B) Quantitative real-time PCR (q-PCR) analysis of *MEG3*, *MEG8*, and *miRNAs*, using fresh skin fibroblasts (SF) of patient 2 and four control neonates. Of the examined *MEGs*, *miR433* and *miR127* are encoded by *RTL1as*. (C) RT-PCR analysis for the formalin-fixed and paraffin-embedded pituitary (Pit.) and the adrenal (Ad.) in patient 2. The bands for *DLK1* are detected in the presence of RT and undetected in the absence of RT, thereby excluding contamination of genomic DNA. (D) Monoallelic *MEG3* expression in the leukocytes of the mother of patient 1. The three cSNPs are present in a heterozygous status in gDNA and in a hemizygous status in cDNA. D: direct sequence. (E) Biparental *RTL1* expression in the placenta of patient 1 and biparental *DLK1* expression in the pituitary and adrenal of patient 2. D: direct sequence; and S: subcloned sequence. In patient 1, genotyping of *RTL1* cSNP (*rs6575805*) using gDNA indicates maternal origin of the "C" allele and paternal origin of the "T" allele, and sequencing analysis using cDNA confirms expression of maternally as well as paternally derived *RTL1*. Similarly, in patient 2, genotyping of *DLK1* cSNP (*rs1802710*) using gDNA denotes maternal origin of the "C" allele and paternal origin of the "T" alleles, and sequencing analysis using cDNA confirms expression of maternally as well as paternally inherited *DLK1*.
doi:10.1371/journal.pgen.1000992.g005

the clinical features in the mother of patient 1 such as short stature and obesity are often observed in cases with upd(14)mat (Table S2). However, the clinical features are non-specific and appear to be irrelevant to the microdeletion involving the IG-DMR, because loss of the paternally derived IG-DMR does not affect the imprinted status [2,26]. Indeed, *MEG3* in the mother of patient 1 showed normal monoallelic expression in the presence of the differentially methylated *MEG3*-DMR. Nevertheless, since the upd(14)mat phenotype is primarily ascribed to loss of functional *DLK1* (Figure S3B) [2,34], it might be possible that the microdeletion involving the IG-DMR has affected a *cis*-acting regulatory element for *DLK1* expression (for details, see Note in the legend for Table S2). Further studies in cases with similar microdeletions will permit clarification of these two points.

In summary, the results show a hierarchical interaction and distinct functional properties of the IG-DMR and the *MEG3*-DMR in imprinting control. Thus, this study provides significant advance in the clarification of mechanisms involved in the imprinting regulation at the 14q32.2 imprinted region and the development of upd(14) phenotype.